

Knight-Field-Enabled Nuclear Spin Polarization in Single Quantum Dots

C. W. Lai, P. Maletinsky, A. Badolato, and A. Imamoglu

Institute of Quantum Electronics, ETH-Zürich, CH-8093 Zürich, Switzerland

(Received 13 December 2005; published 28 April 2006)

We demonstrate dynamical nuclear-spin polarization in the absence of an external magnetic field by resonant circularly polarized optical excitation of a single electron or hole charged quantum dot. Optical pumping of the electron spin induces an effective inhomogeneous magnetic (Knight) field that determines the direction along which nuclear spins could polarize and enables nuclear-spin cooling by suppressing depolarization induced by nuclear dipole-dipole interactions. Our experiments constitute a first step towards a quantum measurement of the Overhauser field.

DOI: [10.1103/PhysRevLett.96.167403](https://doi.org/10.1103/PhysRevLett.96.167403)

PACS numbers: 78.67.Hc, 03.67.Pp, 71.70.Jp

Hyperfine interactions in quantum dots (QD) are qualitatively different than those in atoms: coupling of a single electron-spin to the otherwise well-isolated quantum system of nuclear spins in a QD gives rise to rich physical phenomena such as non-Markovian electron-spin decoherence [1–3]. It has also been proposed that the long-lived collective nuclear-spin excitations generated and probed by hyperfine interactions could have potential applications in quantum information processing [4,5]. Several groups have previously reported QD nuclear-spin cooling using external magnetic fields [6–8]. To achieve dynamical nuclear-spin polarization (DNSP), it has generally been assumed that a small but nonzero external magnetic field is necessary.

Here, we use resonant circularly polarized optical excitation of a single electron or hole charged QD to demonstrate DNSP in the absence of an external magnetic field. We show that optical pumping of the electron spin induces an effective inhomogeneous magnetic (Knight) field that can be more than an order of magnitude larger than the characteristic nuclear dipolar fields, which in turn ensures that DNSP is not suppressed by the latter. Our experiments constitute a first step towards a projective (quantum) measurement of the effective nuclear (Overhauser) field operator [9]: when realized, such a measurement could decrease the uncertainty in the Overhauser field to a level that is smaller than its initial standard deviation, which would in turn suppress nuclear-spin-induced electron-spin decoherence [10].

DNSP is investigated using single self-assembled QDs in gated structures that allow for deterministic charging of a QD [11] with a single excess electron or hole. The InAs quantum dots are grown (by molecular beam epitaxy) 25 nm above a 40 nm heavily doped n^+ -GaAs layer, followed by 30 nm GaAs and an AlAs/GaAs superlattice barrier layer. A bias voltage is applied between the top Schottky and back Ohmic contacts to control the charging state of the quantum dots. The density of quantum dots is below $0.1/\mu\text{m}^2$. In this Letter, data based on two different QDs, labeled as QD-A and QD-B, are analyzed.

Single QDs are studied using a standard micro-photoluminescence (μ -PL) setup that is based on a combination of a solid immersion lens (refractive index $n \approx 2.2$) in Weierstrass configuration and an objective with a numerical aperture of 0.26. A longitudinal (z axis) magnetic field ranging from $B_{\text{ext}} = 0$ to 20 mT is produced by Helmholtz coils positioned around the flow cryostat. The spectroscopy system consists of a 0.75 m monochromator and a cooled CCD camera, providing a spectral resolution of $\sim 30 \mu\text{eV}$. By using a scanning Fabry-Perot interferometer of 62 μeV free spectral range and a finesse ≥ 70 , a spectral resolution $< 1 \mu\text{eV}$ is achieved.

The PL polarization and spin splitting are studied by resonantly exciting a single QD in one of its (discrete) excited (p -shell) states at $T = 5$ K. The PL spectral lines associated with different charging states of a single QD [11] can be identified from the PL intensity contour plot as a function of the bias voltage and emission energy [Fig. 1(a)]. The neutral exciton X^0 line exhibits a fine-structure splitting of $\sim 20 \mu\text{eV}$ (for both QD-A and QD-B) due to the anisotropic electron-hole exchange interaction (AEI). The negatively (positively) charged trion X^- (X^+) emission arising from optical excitation of a single electron (hole) charged QD is red (blue) shifted by ~ 5.5 meV (~ 3.0 meV) with respect to the X^0 line.

The polarization for excitation and detection are denoted as $(\sigma^\alpha, \sigma^\beta)$, where σ^α and σ^β correspond to excitation and detection, respectively. The index α or β assumes one of four values: linear polarization along the $[110](\sigma^y)$, $[1\bar{1}0](\sigma^x)$ crystal axes or circular polarization σ^\pm . The degree of circular polarization is defined as $\rho_c^\pm \equiv (I^\pm - I^\mp)/(I^\pm + I^\mp)$, where I^β denote the intensity of PL under the $(\sigma^\pm, \sigma^\beta)$ configuration. The polarization characteristics of the system is calibrated by the Raman scattering by the longitudinal optical phonon of the GaAs substrate layer and the degree of polarization is found to be better than 98%.

Circularly polarized resonant p -shell pumping of a single electron (hole) charged QD [12,13] generates optically oriented trions with hole (electron) spin $J_z = 3/2$

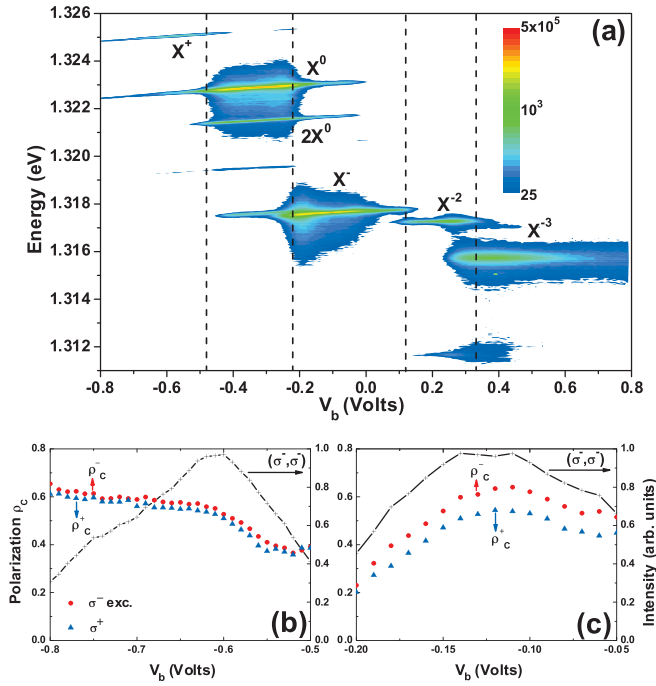


FIG. 1 (color). Photoluminescence from a single charge-tunable quantum dot (QD-A). (a) Contour plot of the PL intensity (log scale) as a function of applied bias voltage under linear polarized excitation and detection $[(\sigma^y, \sigma^y)]$. The excitation is at 1.35615 eV, which corresponds to the p -shell resonance for X^0 ; ~ 40.4 meV above X^0 . (b), (c) Degree of circular PL polarization ρ_c^\pm of PL for X^+ (b) and X^- (c) under (σ^\pm) excitation with energy ~ 35 and 40 meV above X^- and X^+ lines, respectively. ρ_c depends strongly on bias voltage and weakly on pump power (not shown).

($S_z = -1/2$) or $J_z = -3/2$ ($S_z = +1/2$), under σ^+ and σ^- pumping, respectively. The intradot excitation ensures maximal electron (hole) spin preservation during relaxation, which is confirmed by the high degree of circular polarization (ρ_c) of the X^+ (X^-) lines, ranging from $\sim 60\%$ for QD-A [Figs. 1(b) and 1(c)] to $\sim 90\%$ for QD-B (Fig. 2). The initial state of X^+ trion is composed of two holes in a singlet state: σ^+ (σ^-) polarized PL from this state indicates that the optically excited electron is in $S_z = -1/2$ ($S_z = 1/2$) state. For a X^- trion, the initial state is composed of an electron singlet and the PL polarization is determined uniquely by the hole state: σ^+ (σ^-) polarized PL, however, indicates that the electron remaining in the QD after spontaneous emission is in $S_z = 1/2$ ($S_z = -1/2$) state. In both cases polarized PL implies a spin-polarized QD electron, which can in turn polarize nuclear spins via hyperfine interactions [14].

Figure 2(a) shows the spectra of X^- (central energy ~ 1.31634 eV) for QD-B obtained using a scanning Fabry-Perot interferometer under linearly and circularly polarized excitation. Under linearly polarized (σ^y) laser excitation, no fine-structure splitting is observed, confirming the diminished effect of AEI and absence of nuclear-spin polarization. Under circularly polarized (σ^\pm) excitation, spin

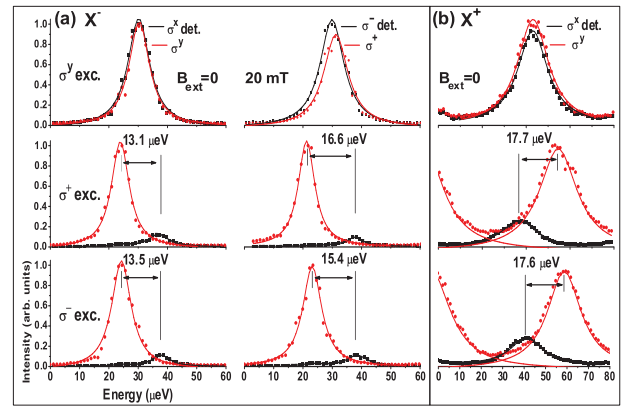


FIG. 2 (color). Spin splitting induced by the Overhauser field. (a) High-spectral-resolution X^- PL spectra measured with a Fabry-Perot scanning interferometer (spectral resolution $\sim 1 \mu\text{eV}$) under $B_{\text{ext}} = 0$ and 20 mT for QD-B. (b) X^+ PL spectra under $B_{\text{ext}} = 0$. Under circularly polarized excitation (σ^\pm), the detection polarization is cocircular (red curves) or cross circular (black) with respect to the pumping polarization. Spin splitting of $\sim 13 \mu\text{eV}$ and $\sim 17 \mu\text{eV}$ are observed under σ^\pm excitation for X^- and X^+ , respectively. For $B_{\text{ext}} = 0$ and linearly polarized excitation (σ^y), colinear or cross-linear polarized PL are detected. In contrast to circular polarization, linear polarization is not preserved. The spin splitting of X^- at $B_{\text{ext}} = 20$ mT under linearly polarized excitation is attributed to Zeeman splitting.

doublets with $\sim 13 \mu\text{eV}$ splitting appear even in the absence of an externally applied magnetic field. The X^- PL peaks that are cocircular with the excitation laser have lower energies for both σ^+ and σ^- excitation [Fig. 2(a)], indicating that the direction of the effective magnetic field responsible for the observed splitting can be changed by switching the electron-spin polarization. For X^+ PL [Fig. 2(b)], this energy sequence is reversed, indicating that the electron spin is polarized in opposite directions in the X^- and X^+ trions, for a fixed circularly polarized laser excitation [8]. Finally, measurements carried out while modulating the excitation polarization between σ^+ and σ^- show that the magnitude of the spin splitting reaches steady state in about ~ 1 sec: when the frequency at which excitation polarization is modulated at 2 Hz, the spin splitting of X^- becomes negligible as the slow nuclear spins can no longer follow the resident electron spin [15]. Based on these observations, we conclude that the spin splitting shown in Fig. 2 is a clear signature of DNSP.

Coupling of a single confined electron to $N \approx 10^5$ nuclear spins in a QD is well described by the Fermi contact Hyperfine interaction [1,16]:

$$\begin{aligned} \hat{H}_{\text{hf}} &= \sum_i A_i |\psi(\mathbf{R}_i)|^2 \hat{\mathbf{S}} \cdot \hat{\mathbf{I}}^i \\ &= -\hbar \sum_i \gamma_i \hat{B}_e^i \hat{I}_z^i + \sum_i \frac{A_i |\psi(\mathbf{R}_i)|^2}{2} [\hat{S}_+ \hat{I}_-^i + \hat{S}_- \hat{I}_+^i], \end{aligned} \quad (1)$$

where $|\psi(\mathbf{R}_i)|^2$ denote the probability density of the electron at location \mathbf{R}_i of the i th nuclear spin; A_i and γ_i are the corresponding hyperfine interaction constant and the gyromagnetic ratio. $\hat{\mathbf{S}}$ and $\hat{\mathbf{I}}^i$ are the electron and nuclear-spin operators, respectively. When the electron is spin polarized via circularly polarized optical excitation under a vanishing external magnetic field, hyperfine interactions play a triple role: first, spin polarized confined electron leads to an inhomogeneous Knight field \hat{B}_e^i seen by each QD nucleus. It should be emphasized that \hat{B}_e^i is an operator that has a finite mean value $\langle \hat{B}_e^i \rangle = B_e \propto \langle \hat{S}_z \rangle$ for a spin-polarized electron. Second, the flip-flop term $\propto \sum_i [\hat{S}_+ \hat{I}_-^i + \hat{S}_- \hat{I}_+^i]$ in Eq. (1) enables nuclear spin pumping along the direction determined by the electron spin, provided that electron is continuously spin polarized by optical excitation and that B_e is larger than local nuclear dipolar fields. Third, the Overhauser field $B_n \propto \sum_i A_i |\psi(\mathbf{R}_i)|^2 \langle \hat{I}_z^i \rangle$ induced by the polarized nuclei on the QD electron results in a spin splitting in PL spectrum that can be detected by high-spectral-resolution spectroscopy as shown in Fig. 2.

It has been argued that an external magnetic field exceeding the local nuclear dipolar fields is necessary to ensure that spin nonpreserving terms in nuclear dipole-dipole interactions are rendered ineffective in depolarizing nuclear spins [17]; this argument is correct only if the Knight field is vanishingly small. If the inhomogeneous nature of electron-nuclear coupling could be neglected, the expectation value of the DNSP generated Overhauser field would be expressed as [16,18–20]

$$\mathbf{B}_n = f \frac{\mathbf{B}^* (\mathbf{B}^* \cdot \langle \mathbf{S} \rangle)}{|\mathbf{B}^*|^2 + \tilde{B}_L^2}, \quad (2)$$

where $\mathbf{B}^* = B_e \hat{\mathbf{z}} + \mathbf{B}_{\text{ext}}$ is the total effective magnetic field seen by the nuclei, $\langle \mathbf{S} \rangle$ is the expectation value of the electron spin, \tilde{B}_L is the effective local field characterizing nuclear-spin-spin interactions [16], and f is a proportionality constant. In the present experiments, similar values of the Overhauser field are observed for $B_{\text{ext}} = 0, 20$ mT (Fig. 2), and 200 mT (measured using a permanent magnet; not shown): the expectation value of the Knight field of a single spin-polarized electron appears to be strong enough to ensure $B_e^2 \gg \tilde{B}_L^2$ and enables significant DNSP without an external magnetic field [21].

Based on Eq. (2), it could be concluded that application of an external field that cancels the Knight field (i.e., $\mathbf{B}^* = 0$) should result in the complete disappearance of DNSP. Figure 3(a) shows the dependence of the observed spin splitting of X^- trion under conditions where the Zeeman splitting due to the external magnetic field (≤ 50 Gauss) is negligible: for this particular QD (A) a dip in spin splitting at $B_{\text{ext}} = -B_e \approx +6$ Gauss is observed under σ^- pumping. Even at this field, however, the spin splitting is only reduced from $\sim 16 \mu\text{eV}$ to $\sim 12 \mu\text{eV}$, indicating that the cancellation of the Knight field B_e by the external field is far from being complete. The minimum in spin splitting is observed at $B_{\text{ext}} \approx -6$ Gauss under σ^+ excitation. The

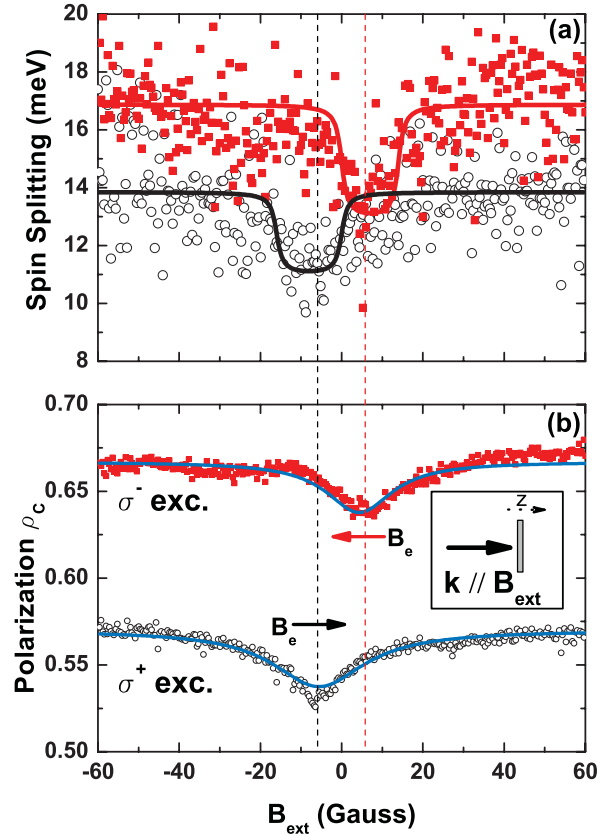


FIG. 3 (color). Spin splitting (a) and PL polarization (b) as a function of applied external magnetic field B_{ext} . Here the spin splitting is determined by a weighted average of the X^- spectral lines measured by the spectrometer. The solid black and red curves in (a) are fits according to the model described in the text. Observation of correlated dips in spin splitting and in polarization as a function of B_{ext} suggests an average Knight field $B_e \approx 6$ Gauss seen by the nuclei. Blue curves in the polarization data shown in (b) are fits obtained from Eq. (3), using averaged values of the data in (a). Under σ^+ (σ^-) excitation, B_e is parallel (antiparallel) to the wave vector \mathbf{k} of laser excitation. The schematic in the inset of (b) sketches the orientations of the laser wave vector and the external magnetic field.

observed minima, which gives the average value of the Knight field B_e , ranges from ± 6 Gauss to $\sim \pm 30$ Gauss depending on the degree of PL polarization, pumping intensity and the QD that is studied. The measured values indicate a time-averaged electron-spin polarization that ranges between 3% and 30%. A fully polarized electron spin would have given rise to a Knight field that is between 100 and 200 Gauss; the uncertainty here is due to our lack of knowledge of the confinement length scale and composition of the QD. The fact that the electron-spin polarization is less than that of the PL is expected given the processes such as cotunneling that randomize the resident electron spin.

The principal reason for the small reduction in DNSP at $B_{\text{ext}} = \pm 6$ Gauss is the inhomogeneity of the Knight field, which ensures that the condition $\mathbf{B}^* = 0$ is satisfied only

for a small class of nuclei at any given B_{ext} : provided $B_e \gg \tilde{B}_L$, the majority of the nuclei experience negligible change in depolarization, keeping the overall spin-splitting nearly unchanged. To demonstrate the role of Knight field inhomogeneity in the data presented in Fig. 3(a), a fitting procedure is carried out where an in-plane Gaussian electron wave function $|\psi(\mathbf{R}_i)|^2 \propto \exp[-(x_i^2 + y_i^2)/l^2]$ is used together with Eq. (2) to estimate the total contribution of the different classes of QD nuclei. The choice of a maximum Knight field of 15 Gauss ($B_e \approx 6$ Gauss), $\tilde{B}_L = 1.1$ Gauss and $l = 20$ nm gives a reasonable description of the experimental data [solid curves in Fig. 3(a)], even though coupling to a single (effective) nuclear species ($A_i = A$) is assumed.

Remarkably, a dip in the degree of PL polarization is also observed for the same B_{ext} [Fig. 3(b)]: this is at first surprising since polarization of the X^- trion line is solely determined by the hole-spin and a direct interaction between the heavy-hole and the nuclei is unlikely to be strong enough [22] to lead to the observed dependence. A possible explanation is based on AEI: after the resonant excitation of the QD, the electron excited into a p -shell state is expected to tunnel out into the n -doped GaAs layer in sub-psec time scale [23]. After tunneling, the QD is neutral and the remaining electron-hole pair is subject to AEI which rotates the electron-hole spin [24]. This coherent rotation is then interrupted by reinjection of another electron from the n -doped GaAs layer into the QD s shell to form a ground-state electron singlet in $\tau_t \sim 5$ –20 psec, as required by the charging condition. Because tunneling is a random process, the post-tunneling hole-spin state is partially randomized and leads to a finite ρ_c . The Overhauser-field competes with the exchange interaction; a reduction in DNSP will therefore lead to a reduction in ρ_c as depicted in Fig. 3(b). The PL polarization in the presence of an Overhauser shift ($\hbar\Omega_{\text{hf}} \propto B_n$) and AEI can be approximated as [25]:

$$\rho_c = \frac{1 + \Omega_{\text{hf}}^2 \tau_t^2}{1 + (\Omega_{\text{hf}}^2 + \omega_{\text{ex}}^2) \tau_t^2}, \quad (3)$$

provided other spin relaxation processes are neglected. Fitting the polarization $\rho_c(X^-)$ with the measured spin splitting in Fig. 3(a) taken for QD-A, $\tau_t = 30$ psec is obtained [26]. For QD-B [Fig. 2(a)], $\tau_t \approx 10$ psec is obtained for $\rho_c(X^-) \approx 90\%$ using Eq. (3). Below saturation, a reduction in the excitation power results in a decrease in both spin splitting and ρ_c : this observation corroborates the model described by Eq. (3).

The electron (spin) exchange with the n -doped GaAs layer also explains how QD electron-spin pumping is achieved in a negatively charged QD: irrespective of the preexcitation electron state, the sequential tunneling ensures that the QD ends up in a trion state where the electrons form an s -shell singlet. Preservation of hole-

spin in these QDs then implies that the post-recombination electron is always projected into the same spin-state.

Some of the open questions that warrant further investigation include the reasons for relatively low level of DNSP where only $\sim 10\%$ of the QD nuclei appear to be polarized; differences in the magnitude of DNSP among the four different nuclear species present in self-assembled QDs; and the role of quadrupolar interactions enhanced by the strain [27]. By using differential transmission measurements [28], it should be possible to enhance the accuracy with which the Overhauser field can be measured by at least an order of magnitude.

We thank J. Dreiser for assistance and K. Karrai, O. Krebs, X. Marie, G. Salis, G. Giedke, J. Taylor, M. Lukin, D. Bulaev, D. Loss, and A. Efros for discussions. This work is supported by NCCR-Nanoscience.

-
- [1] A. V. Khaetskii *et al.*, Phys. Rev. Lett. **88**, 186802 (2002).
 - [2] A. C. Johnson *et al.*, Nature (London) **435**, 925 (2005).
 - [3] F. H. L. Koppens *et al.*, Science **309**, 1346 (2005).
 - [4] J. M. Taylor *et al.*, Phys. Rev. Lett. **90**, 206803 (2003).
 - [5] J. M. Taylor *et al.*, Phys. Rev. Lett. **91**, 246802 (2003).
 - [6] D. Gammon *et al.*, Science **277**, 85 (1997).
 - [7] K. Ono and S. Tarucha, Phys. Rev. Lett. **92**, 256803 (2004).
 - [8] B. Eble *et al.*, cond-mat/0508281.
 - [9] D. Stepanenko *et al.*, Phys. Rev. Lett. **96**, 136401 (2006).
 - [10] W. A. Coish and D. Loss, Phys. Rev. B **70**, 195340 (2004).
 - [11] R. J. Warburton *et al.*, Nature (London) **405**, 926 (2000).
 - [12] A. S. Bracker *et al.*, Phys. Rev. Lett. **94**, 047402 (2005).
 - [13] M. E. Ware *et al.*, Phys. Rev. Lett. **95**, 177403 (2005).
 - [14] A. Imamoglu *et al.*, Phys. Rev. Lett. **91**, 017402 (2003).
 - [15] Suppression of the DNSP also leads to a drop in ρ_c by more than 40%, consistent with Eq. (3).
 - [16] D. Paget *et al.*, Phys. Rev. B **15**, 5780 (1977).
 - [17] D. Gammon *et al.*, Phys. Rev. Lett. **86**, 5176 (2001).
 - [18] F. Meier, *Optical Orientation* (North-Holland, Amsterdam, 1984).
 - [19] M. I. Dyakonov and V. I. Perel, Sov. Phys. JETP **36**, 995 (1973).
 - [20] V. L. Berkovits *et al.*, Phys. Rev. B **18**, 1767 (1978).
 - [21] We measured the stray field in our setup to be 0.5 ± 0.1 Gauss; this field makes an angle of $\sim 25^\circ$ with the optical axis.
 - [22] E. I. Gryncharova and V. I. Perel, Sov. Phys. Semicond. **11**, 997 (1977).
 - [23] J. M. Smith *et al.*, Phys. Rev. Lett. **94**, 197402 (2005).
 - [24] S. Laurent *et al.*, Phys. Rev. Lett. **94**, 147401 (2005).
 - [25] E. L. Ivchenko, Pure Appl. Chem. **67**, 463 (1995).
 - [26] As shown in Fig. 1(b), QD-A exhibits an asymmetric polarization under σ^\pm pumping: the origin of this asymmetry is not clear. We observed no such asymmetry for QD-B.
 - [27] C. X. Deng and X. D. Hu, Phys. Rev. B **71**, 033307 (2005).
 - [28] A. Hogege *et al.*, Appl. Phys. Lett. **86**, 221905 (2005).